Nanocellulose/polymer multilayered thin films: tunable architectures towards tailored physical properties

Clélia Martin and Bruno Jean

KEYWORDS: Nanocellulose, Polymer, Layer-by-layer assembly, Architecture, Properties

SUMMARY: This article reviews development of nanocellulose/polymer multilayered films. The layer-by-layer assembly technique has been used for about a decade to build thin films composed of alternating layers of either cellulose nanocrystals (CNCs) or cellulose nanofibrils (CNFs) with different polymers (e.g. synthetic polycations or neutral biopolymers). We show that the resulting architectures, which have been probed using various surface-sensitive techniques, are highly tunable and depend on the individual properties of the constituents, the interaction forces between the nanocellulose and the polymer and the deposition method parameters. The composition and morphology of these fully biobased or hybrid fossil/natural nanocomposite films can be precisely tailored to achieve different physical properties that have been investigated. We describe how high performance thin films and coatings with advanced functionalities can be designed and potentially used in the fields of permeation membranes, bioenergy production, drug delivery, flexible electronics, controlled adhesion or optical protective coatings.

ADDRESSES OF THE AUTHORS: Clélia Martin (clelia.martin@cermav.cnrs.fr) and Bruno Jean (bruno.jean@cermav.cnrs.fr) Centre de Recherches sur les Macromolécules Végétales (CERMAV-CNRS)¹, BP53, 38041 Grenoble cedex 9, France

Corresponding author: Bruno Jean

The ongoing progress towards the development of biosourced materials able to replace petroleum-derived products requires the use of nature-based building blocks displaying several key characteristics. Among these, one can cite the ability to be produced at an industrial scale from an abundant natural resource, non competition with food sources and the aptitude to tunable structural organizations. Nanocellulose, comprising both cellulose nanocrystals (CNCs) and cellulose nanofibrils (CNFs), fulfills most of these conditions. Indeed, nanoparticles extracted from an almost inexhaustible resource now benefit from the development of industrialscale productions motivated by the need for new markets for the wood natural resources. Further, nanocellulose exhibits valuable properties like low density, high mechanical strength, tunable aspect ratio morphology, and broad chemical modification capacity along with general features of nanoscale objects including very large specific surface area. In this framework, various research groups worldwide have aimed at taking advantage of the exceptional intrinsic

properties of nanocellulose coupled with the structuration enabled by the layer-by-layer (LbL) assembly technique to design nanocellulose/polymer thin films and coatings with advanced functionalities. Generally speaking, the socalled LbL assembly, first introduced by Iler (1966) and developed by Decher et al. in the nineties (1992; 1997), is a simple, versatile, environmentally friendly and low-cost method to build multilayered films incorporating different components with a tunable internal organization nanometer scale. First developed polyelectrolytes, the method has been extended to various constituents such as small organic molecules or inorganic compounds, biomacromolecules like DNA or proteins and colloids like clays, carbon nanotubes or latexes (Decher et al. 2012). Interaction forces responsible for the film buildup and cohesion include electrostatics, hydrogen bonding, hydrophobic interactions, covalent linkages, π - π interactions etc. One key advantage of the LbL technique is that it can be applied to solvent accessible surfaces of almost any kind and any shape including colloids, textile or paper.

The first study on nanocellulose/polymer multilayered films dates back to 2005 and was reported by the team of Nicholas Kotov, from the University of Michigan, a leading group in the field of layer-by-layer assembly research (Podsiadlo et al. 2005). Since then, the nanocellulose/polymer research field has attracted interest mainly from the nanocellulose community and new developments aim at targeting applications in the fields of separation membranes, flexible electronics, bioenergy and advanced optical coatings.

The present review article describes the state of the art in the nanocellulose/polymer LbL film research field. In a first part, the various building blocks and systems investigated and the different deposition methods are defined. The second and third parts are devoted to the presentation of general trends and of the different triggers that can be used to finely tune the architecture of the film, including the modulation of the interaction forces and the deposition parameters. The physical properties of nanocellulose/polymer thin films are finally presented with examples of advanced film functionalities.

Nanocellulose/polymer multilayers: building blocks and LbL assembly

Two types of nanocellulose

Nanocellulose is a generic terminology that refers to two different cellulose nanoparticles: cellulose nanocrystals and cellulose nanofibrils.

CNCs are rodlike cellulose crystals generated from the removal of amorphous regions of purified cellulose microfibrils by acid hydrolysis. Their preparation is generally based on the protocol described by Revol et al. (1992). Dimensions of CNCs both depend on the cellulose source and on the hydrolysis conditions with

¹ *Affiliated with Université de Grenoble, member of the Institut de Chimie Moléculaire de Grenoble (ICMG) and member of the PolyNat Carnot Institute

cross-sections ranging from 3-30 nm and lengths between 100 nm and several micrometers (Habibi et al. 2010; Eichhorn 2011; Klemm et al. 2011). Sulfuric acid hydrolysis converts part of the surface hydroxyl groups into negatively charged sulfate ester groups, providing colloidal stability to CNCs in aqueous media due to electrostatic repulsions and leading to their spectacular self-organization properties in liquid crystalline phases (Revol et al. 1992). The charge density of CNCs is about 0.5 e/nm² (0.2-0.5 meq/g). CNCs most widely used in the buildup of multilayered films have been extracted from cotton with average dimensions of 130×26×6 nm³ and a broad size distribution (Elazzouzi-Hafraoui et al. 2008). Tunicin nanocrystals extracted from the sea animal tunicate have also been occasionally employed. These CNCs are 10-20 nm in width and 500-2000 nm in length, thus exhibiting a much larger aspect ratio than cotton CNCs.

CNFs are composed of liberated semi-crystalline microfibrils, normally produced using high-pressure homogenization of wood fibers in water. First introduced by Turbak et al. (1983), new methods for the production of smaller diameter and more homogeneous CNFs have since been developed using a combination of enzymatic and mechanical pretreatment followed by high-pressure homogenization (Pääkkö et al. 2007). Unlike the rigid and highly crystalline CNCs, CNFs contain both amorphous and crystalline regions generating flexibility and possible entanglements. As far as multilayered films are concerned, negatively charged carboxymethylated

CNFs resulting from the carboxymethylation of the original wood fibers were generally used and, unless otherwise stated, CNF in this review will refer to such particles. Carboxymethylated CNFs have cross-sections between 5 and 15 nm and lengths that exceed 1 µm. Their charge density is around 0.5 meq/g. Alternatively, carboxylated CNFs generated by TEMPO oxidation and leading to highly charges particles were employed. Cationic CNFs (catCNF) resulting from the reaction of CNFs with N-(2,3 epoxypropyl)trimethylammonium chloride under alkaline conditions were also used.

In this review article, the terminology being approved by the Technical Association of the Pulp and Paper Industry (TAPPI), the International Organization for Standardization (ISO) and the Canadian Standards Association (CSA), which is cellulose nanocrystals (CNCs) and cellulose nanofibrils (CNFs) will be used. However, in the literature, cellulose nanocrystals have also been referred as cellulose microcrystals, cellulose whiskers, cellulose nanowhiskers (CNW) nanocrystalline cellulose (NCC) while the terms microfibrillated cellulose (MFC) and nanofibrillated cellulose (NFC) were used to designate cellulose nanofibrils.

Various compositions based on different interaction forces CNCs and CNFs in conjunction with polymers are ideal building blocks for the construction of multilayers as long as attractive interactions can take place between both components. On one hand, both types of nanocellulose

Table 1 - Various nanocellulose/polymer systems studied in the literature. Here CNF refers to carboxylated cellulose nanofibrils. aCNF-DOPA stands for dopamine functionalized CNFs.

Nanocellulose	Polymer	Reference
CNC from cotton	PDDA	(Podsiadlo et al. 2005; Sui et al. 2010)
CNC from cotton	PAH	(Cranston, Gray 2006a; 2006b; 2008; Jean et al. 2008; Cranston et al. 2010; Moreau et al. 2012)
CNC from cotton	PEI	(Kan, Cranston 2013)
CNC from cotton	Xyloglucan	(Jean et al. 2009; Cerclier et al. 2010; Cerclier et al. 2011)
CNC from cotton	Cationic xylan	(Dammak et al. 2013)
CNC from ramie	DHP	(Hambardzumyan et al. 2011)
CNC from eucalyptus	Chitosan	(de Mesquita et al. 2010)
CNC from eucalyptus	Collagen	(de Mesquita et al. 2011)
CNC from tunicate	PEI	(Podsiadlo et al. 2007)
CNF	PEI	(Aulin et al. 2008; Wågberg et al. 2008; Aulin et al. 2009; Aulin et al. 2010; Cranston et al. 2011; Karabulut, Wågberg 2011; Aulin et al. 2013)
CNF	PAH	(Wågberg et al. 2008)
CNF	PDDA	(Wågberg et al. 2008; Eronen et al. 2012)
CNF	PVAm (+SiO2)	(Eita et al. 2011)
CNF	Cationic starch	(Eronen et al. 2012)
CNF	Cationic CNF	(Aulin et al. 2010; Eronen et al. 2012)
CNF	NIPAAm-based cationic copolymer	(Utsel et al. 2010)
CNF	polyaniline	(Shariki et al. 2011)
CNC from cotton	Cationic CNF	(Olszewska et al. 2013)
CNF-DOPA ^a	PEI	(Karabulut et al. 2012)

carry negative surface charges and can be associated with polycations via electrostatic interaction forces. In this synthetic polycations like poly(allyamine hydrochloride) (PAH), poly(diallyldimethylammonium chloride) (PDDA), and polyethyleneimine (PEI), or natural positively charged polymers like chitosan, cationic starch or collagen have been used. On the other hand, different research teams took advantage of the nonelectrostatic interactions that can take place between nanocellulose and biopolymers like xyloglucan or lignin. Pure nanocellulose films were also occasionally built using cationic CNFs associated either with carboxylated CNFs or cotton CNCs. Finally, derivatized CNFs or thermosensitive copolymers were also used to achieve advanced functionalities. Table 1 lists all the nanocellulose/polymer multilayered systems that have been studied up to now.

Film building using the Layer-by-layer assembly

Nanocellulose/polymer multilayered films described in the literature were built using the LbL deposition technique. The deposition was achieved on various substrates but silicon wafers are the most commonly used solid surfaces. As shown in Fig 1, providing attractive forces can develop between the components, the basic principle of the LbL assembly is the alternate deposition of the constituents from solutions or dispersions with intermediate rinsing steps to remove loosely linked species. The cycle can be repeated as many times as wanted to reach the desired number of layers. Three deposition methods have been developed for the preparation of LbL assembled films: dip-coating, spin coating and spraying. Dip-coating or dipping consists in the immersion of the substrate (generally a silicon wafer or a glass plate) in the different components solutions or dispersions. The dipping time must be long enough to reach adsorption equilibrium and, when appropriate, overcompensation of the surface charges. Spin-coating and spraying significantly reduce the deposition time, which is typically 5 seconds compared to 5-15 min for dipping. Contrary to thermodynamically controlled dipcoating, due to the action of centrifugal, viscous and shear forces, spraying and spin coating are also mechanically controlled (Cranston, Gray 2009). The morphology of multilayers will thus be different depending on the method used.

In the following, the term bilayer will refer to the successive deposition of one nanocellulose layer and one polymer layer. Additionally, the notation $(nanocellulose/polymer)_n$ designates a multilayered film constituted by n nanocellulose/polymer bilayers.

Characterization techniques

The architecture of nanocellulose/polymer thin films is defined by several parameters: the total film thickness, and the composition, roughness, porosity and thickness of each sublayer constituting the multilayer. These parameters are influenced by the components' individual characteristics, the type and strength of the interactions between the nanocellulose and the polymer, and the deposition method. The structural details of such films

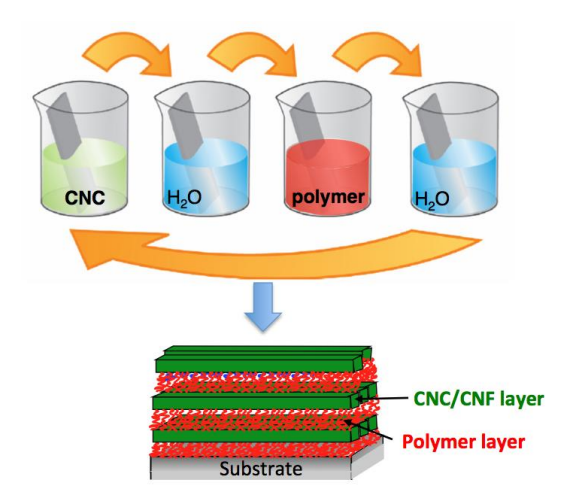


Fig 1. Layer-by-layer assembly of (nanocellulose/polymer) thin films by dip-coating.

can be investigated by combining various surface sensitive techniques such as atomic force microscopy (AFM), scanning electron microscopy (SEM), ellipsometry, quartz-crystal microbalance with dissipation monitoring (QCM-D), dual polarization interferometry (DPI), stagnation point adsorption reflectometry (SPAR) and neutron reflectivity (NR).

General trends

Film growth

CNCs and CNFs in conjunction with various polymers have been successfully employed to build thin multilayered films. Indeed, as long as interaction forces between the nanocellulose and the polymer are strong enough, unlimited growth is observed for films composed of either class of cellulose nanoparticle. However, due to differences in size, aspect ratio, charge density and flexibility, the use of CNCs or CNFs results in different film buildup behaviors.

For CNC/polymer films, a linear growth is generally observed. An example of such a behavior is shown in Fig 2A. Films with up to 140 bilayers (Podsiadlo et al. 2007) were assembled and the total film thickness ranged from several nanometers for a few bilayers up to 1 μ m. Using CNCs, the film thickness increment (defined as the average thickness increase upon deposition of a CNC/polymer bilayer) varies in a wide range, from 2 nm (Cranston and Gray 2006a) to 39 nm (Kan and Cranston 2013), depending on the associated polymer and the experimental conditions.

For CNF/polymer films, the growth is more dependent on polymer properties. For example, as shown in *Fig 2B*, the thickness's increase for CNF/PEI films is low for the first few layers prior to reaching an increased linear growth rate, whereas CNF/PAH multilayers exhibit a linear growth rate from the initiation of construction. Exponential growth has also occasionally been observed (Karabulut, Wågberg 2011). Below 20 deposited bilayers, growth rates between 2 and 12 nm per bilayer were measured for CNF based films, which is usually inferior to growth rates observed with CNCs. However, thickness as high as 5.8 μm were reported for (PEI/NFC)₁₅₀ films (Karabulut and Wågberg 2011).

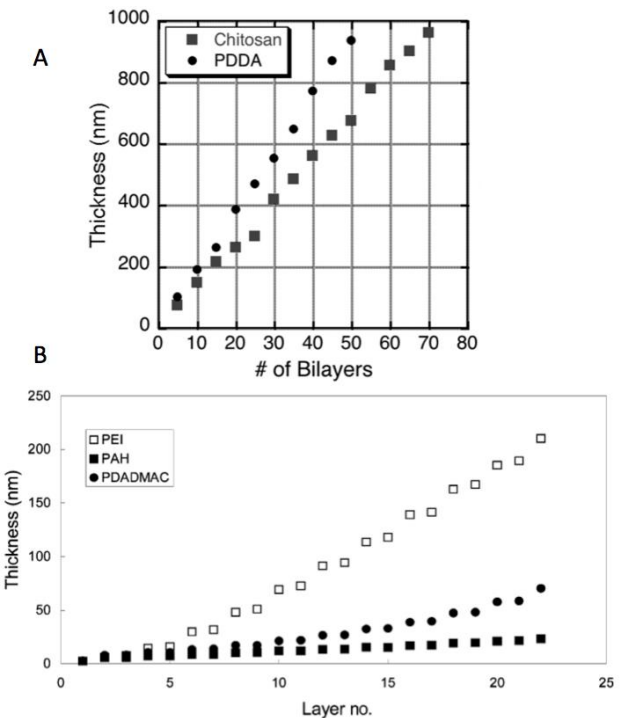


Fig 2 - A) Film thickness vs. bilayer number for chitosan/CNC and PDDA/CNC LbL films. B) Film thickness vs. number of layers of multilayered films from CNF and, respectively, PEI, PAH, and PDADMAC, measured by ellipsometry. No extra salt was added, and the pH was between 7 and 8 in all the treatment steps. Reprinted with permission from Sui et al. 2010 and Wågberg et al. 2008. Copyright 2010 and 2008 American Chemical Society.

Surface morphology

The surface morphology of the film strongly depends on the aspect ratio of the nanocellulose particles. When low aspect ratio CNCs extracted from cotton or eucalyptus are used, a uniform and dense surface coverage is achieved. Conversely, rigid high aspect ratio tunicin CNCs give rise to cellulose layers with a much lower nanoparticle density, resulting in a porous structure similar to that of a "flattened matchsticks pile" (Podsiadlo et al. 2007). High aspect ratio but flexible CNFs tend to give open fibrillar networks (Aulin et al. 2008; Wågberg et al. 2008). These various surface morphologies are illustrated in *Fig 3*.

Nanocellulose multilayers have relatively smooth surfaces since their root-mean-square roughness (determined by AFM) remain below 10 nm. The use of high aspect ratio CNCs such as those extracted from tunicin leads to rougher surfaces (Podsiadlo et al. 2007). It has been shown that the deposition method influences the final roughness. Spin coated films exhibit a constant roughness whereas a small increase has been noticed in the case of dip coated (CNC/PAH) multilayers (Cranston, Gray 2006a; Jean et al. 2008). It also seems that the adsorption of dual CNC layers gives higher roughness than monolayers (Jean et al. 2009).

Due to their anisotropic shape, CNCs and CNFs are good candidates for the preparation of oriented films that could herald a new class of thin films with enhanced mechanical strength and specific optical properties. Various strategies can be employed for building

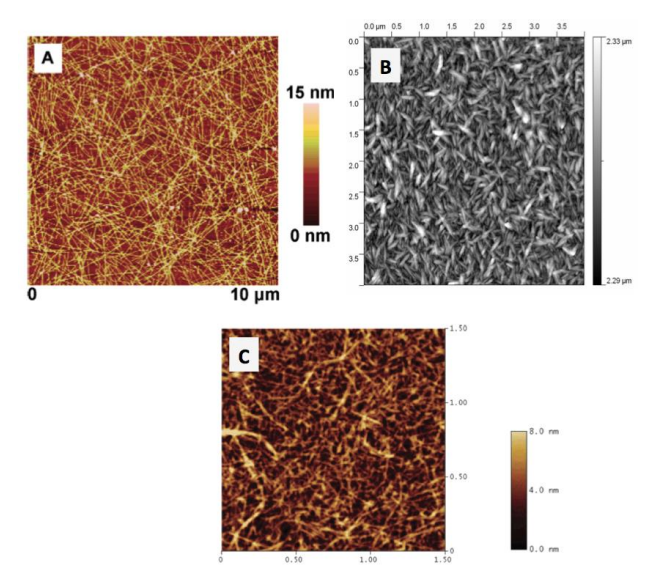


Fig 3 - AFM topography images of A) single PEI/tunicate CNC bilayer with 1 min PEI and instantaneous tunicate immersions. B) single PAH/cotton CNC bilayer and C) single PEI/NFC bilayer (no additional electrolyte has been added) deposited on Si wafers. Reprinted with permission from Podisadlo et al. 2007 (A) Jean et al. 2008 (B) and Wågberg et al. 2008 (C). Copyright 2007 and 2008 American Chemical Society.

oriented CNCs multilayers. Jean et al. took advantage of the bulk self-organization of CNCs into chiral nematic phases to transfer the orientation to the films (Jean et al. 2008). By dipping the substrate in a self-organized suspension, a substantial uniaxial orientation was indeed observed by AFM and further evidenced by Fourier transform of the images. Similarly, by dipping a silicon substrate in a 9 wt% chiral nematic CNC suspension under strong magnetic field (7T), Cranston and Gray (2006b) could observe orientation of the adsorbed nanorods. However, a long exposure time of 24h in the field was required. Alternatively, CNCs orientation can stem from the shear flow that occurs during the spin coating deposition (Cranston, Gray 2006a). This technique allows for a radial orientation of the nanorods.

Sensitivity of the architecture of the film to various parameters

Adsorption kinetics and final architecture of multilayered films strongly depend on the individual properties of the nanocellulose suspensions and polymer solutions, on the type and strength of nanocellulose/polymer interactions and on the deposition conditions and methods. A large variety of parameters can thus be tuned to tailor the characteristics of the thin films. In this section, we will detail some key parameters that strongly influence the interaction forces between the film's building blocks and hence its internal structure.

Structural tunability in polycation/nanocellulose films

Two general rules

From the analysis of results described in the literature, it can be concluded that the conformation of the polymer associated with the nanocellulose has a strong influence on the films architecture and significantly governs the adsorption of the nanoparticles. Two main situations can be distinguished:

- 1. when the polymer chains are in an extended conformation, they tend to form thin and dense layers and the consecutive nanocellulose adsorption is characterized by low adsorbed amounts and thin layers. This is the case when linear polycations with high charge density and/or low ionic strength solutions are used.
- 2. when the polycation rather adopts a coiled conformation, it adsorbs as thick swollen layers, which favors the adsorption of thick nanocellulose layers with a high adsorbed amount. This situation occurs when branched polycations or linear polycations with low charge density and/or high ionic strength conditions are chosen.

Both cases were observed and described by Wågberg et al. (2008) who compared the build-up of CNF/polymer multilayers using different types of polycations and different ionic strengths of polyelectrolyte solutions. The adsorption of a polycation with a coiled threedimensional structure, which can be obtained using branched PEI or linear PDDA and PAH at high salt concentration, leads to thick CNF layers. Conversely, the use of highly charged linear polycations results in the formation of thin CNF layers. Similar effects were reported by Aulin et al.: at high pH values, low charged PEI form thick layers that incorporate a large amount of water, leading to an increase in the adsorbed amount of CNFs. The adsorption of a thin and dense PEI layer at low pH conversely gives rise to a decrease in the adsorbed amount of PEI/CNF bilayers (Aulin et al. 2008). As shown by Eronen et al. (2012) the low charge density and high molecular weight cationic starch adsorbs with a coiled conformation favoring high adsorbed amounts of CNFs. Conversely, thin PDDA layers arising from the high charge density and linearity of this polymer result in low adsorbed amounts in the films.

The same rules apply to CNCs. For example, using a 1 M NaCl PAH solution results in thicker PAH/CNC films with a thickness increment around 15-20 nm/bilayer, compared to the 7-9 nm/per bilayer value found using a salt free PAH solution (Jean et al. 2008; Moreau et al. 2012). Consistently, a high thickness increment per bilayer of 39 nm was found for PEI/CNC films where the branched nature of PEI allows for higher adsorbed mass of CNCs as its chains can slot into the CNC layer toward the surface, providing more cationic charges for even more interactions with CNCs (Kan, Cranston 2013). However, in contradiction with the aforementioned results, Podsiadlo and coworkers (2007) reported that the nature of the polyelectrolyte has no influence on the growth of tunicate CNC/polycation multilayers. Indeed, these authors found similar results (i.e. an average thickness increase per bilayer equal to 7 nm) when CNCs are associated with linear polycations like PAH, PDDA, chitosan or with branched polymers like PEI.

Double layer versus single layer

Jean et al. (2008) and Moreau et al. (2012) reported that CNCs adsorb as a double layer when associated in multilayers with PAH in presence of 1M NaCl in the

polymer solution (Fig 4B). NR data especially reveal the presence of this dual layer shown by the observation of a Bragg peak and also demonstrate that the two cellulose layers have different adsorption densities: 50% for the dense bottom layer and 25% for the top one (Jean et al. 2008). The first CNC monolayer adsorbs onto the PAH sublayer due to electrostatic interactions by complex formation and counterion release. In the presence of salt, due to charge screening, PAH adopts a partially swollen conformation favoring polymer loops and tails that can interpenetrate the first CNC layer, making some cationic charges available for the adsorption of a more dilute second CNC layer. Concomitantly, the adsorption of this second layer is strongly promoted by the gain of entropy associated with counterions release. Hydrogen bonding between the CNC layers can also develop, especially upon drying, and strengthen the overall cohesion of the film. Considering the surface charge density of fully ionized PAH to be 3.00-3.75 e/nm² (depending on the hydration of the film) (Cranston and Gray 2006) and that of sulfated CNCs to be in the range 0.5-0.6 e/nm², charge reversal, which is usually a prerequisite for multilayer build-up, can never be achieved. However, since CNCs exhibit a high thickness compared to polymer layers, adsorption of parallelepipedic CNCs can be considered to occur mostly through interactions between the charges located on one side of the nanocrystals, leaving negative charges on the opposite upper side available for interactions with the next polycation layer. It can thus be considered that a pseudo geometrical charge reversal can be obtained even if a non-stoichiometric charge ratio is reached (Oksman in press).

In contrast, when salt-free polycation solutions are used, the polymer chains tend to adopt an extended conformation due to repulsions between charged monomers, leading to the adsorption of thin and flat polymer layers. In this configuration, as shown in the case of PAH/CNCs and chitosan/CNCs films, a single CNC layer adsorbs through electrostatic interactions between the available polycation charges and the anionic

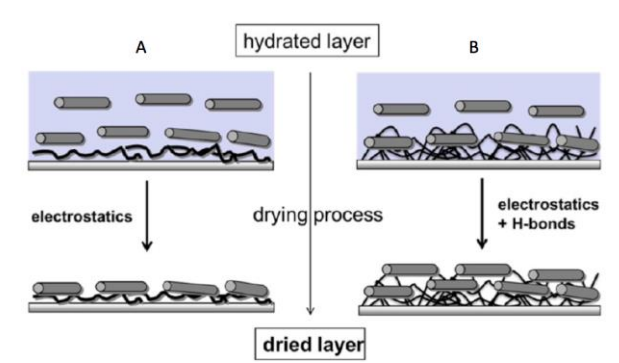


Fig 4 - Schematic representation of the CNC (gray rods) adsorption process onto a single layer of PAH (black segments) previously deposited from a solution A) without and B) with salt ions. Without salt, PAH chains adsorb in a plane configuration, whereas in the presence of salt ions, they adsorb in a coiled conformation. After the drying step, CNCs adsorbed as a single layer in A) and as a double layer in B). Reprinted with permission from Moreau et al. 2012. Copyright 2012 American Chemical Society.

groups on one side of the CNC (de Mesquita et al. 2010; Moreau et al. 2012) (*Fig 4A*). As aforementioned, subsequent adsorption of polycations is possible thanks to geometrical charge reversal.

Effect of nanocellulose charge

Eronen and coworkers (2012) studied the effect of the fibrils charge density using highly charged TEMPO oxidized CNFs and unmodified low charged CNFs. Multilayer formation was successful with both types of CNFs when combined with PDDA or cationic starch. However, the increase in sensed mass by QCM-D after the total 7-9 layer addition was systematically higher with highly charged CNFs. Higher energy dissipation values have been recorded with high charged fibrils, evidencing a more viscoelastic and extended nature of these CNFs compared to low charged CNFs. Whatever the polycation, the adsorption of low charged CNFs slowed down after the 7th bilayer, due to both lower charge and increased size of the fibrils. Using DPI, Aulin et al. could show that an increase in the electrolyte concentration of the CNF suspension reduced but did not totally prevent the adsorption of CNFs onto PEI. Although a limited electrolyte concentration range was tested (1-100 mM NaI), this result suggests that a nonelectrostatic driving force might contribute to the adsorption of CNFs (Aulin et al. 2008).

Nonelectrostatic interactions in nanocellulose/ biopolymer films

A large majority of LbL nanocellulose multilayered films have been built through electrostatic interactions. Nevertheless, film growth can also be achieved using other attractive forces such as hydrogen bonding or hydrophobic interactions. In order to build fully biosourced nanocomposites, CNCs can be associated with xyloglucan, a neutral biopolymer that constitutes the major hemicellulose in the primary cell wall of dicotyledonous plants (Jean et al. 2009; Cerclier et al. 2010; Cerclier et al. 2011; Cerclier et al. 2013). XG chains exhibit a strong affinity for cellulose and this strong adsorption is thought to arise from concomitant van der Waals forces, polar interactions and hydrogen bonding (Hanus, Mazeau 2006). The XG concentration is of prime importance for the successful growth of these green multilayers (Cerclier et al. 2010). At high XG concentration (entangled semidilute regime), the films reached a plateau after the deposition of 2 or 4 bilayers, whereas at low XG concentration (unentangled semidilute regime) an unlimited growth was observed. At low concentration, the XG chains adsorb in a flat conformation and thus interact with both upper and lower CNC layers. At higher XG concentration, a greater amount of polymer is adsorbed and the probability for a XG chain to be linked with both upper and lower CNC layer is low. The architecture of XG/CNC multilayers is thoroughly dependent on the deposition method used. When the dip-coating process is chosen, the (XG/CNC) multilayer consists of the periodic repetition of a single layer of CNC having a 45% volume fraction and a thin layer of xyloglucan (Jean et al. 2009). On the contrary, spin-coated (XG/CNC) films appeared to be less stratified and the thickness increase per bilayer of 16.4 nm suggests the adsorption of 2 layers of CNC plus a thin layer of XG (Cerclier et al. 2011).

Another type of film was built by intercalating PAH layer between XG/CNC complexes layers (Cerclier et al. 2013). In this case, the authors took advantage of both the interactions between XG and the CNCs and the electrostatic interactions between PAH and the negatively charged CNCs. NR data reveal that (XG/CNC) and (XG-CNC/PAH) multilayers of similar thicknesses have equal XG contents but different CNC contents: the XG/CNC ratio is equal to 0.89 for the first model and to 2.15 for the second one. Hence, the concentration of unbound XG is higher in the second model and this leads to a looser structure with a less crossed-linked CNC/XG network.

De Mesquita et al. (2011) investigated CNC/collagen multilayers in which hydrogen bonding seems to play an important role in the buildup. Surprisingly, the thickness of both collagen and CNC layers, 2.5 nm and 6 nm, respectively, were independent of the electrolyte concentration in the collagen solution (0, 20 or 100 mM NaCl). The successful buildup may arise from concomitant electrostatic interactions (collagen is slightly positively charged in the pH conditions used for the LbL assembly) and hydrogen bonds between amide groups of collagen and hydroxyl groups of CNCs.

All-cellulose multilayers

Several researchers took advantage of the surface derivatization of CNFs into cationically modified CNFs (catCNF) to build pure cellulose nanoparticle LbL films composed of either anionic CNFs and catCNFs (Aulin et al. 2010; Eronen et al. 2012) or catCNFs and anionic CNCs (Aulin et al. 2010; Olszewska et al. 2013). For the first system, SPAR data show that the adsorbed amount of cationic/anionic CNF increases slowly but linearly with increasing number of layers, suggesting successful buildup. However, the total adsorbed amount of a fivebilayer film, about 6 mg/m², is considerably lower than the 30 mg/m² adsorbed amount for a (PEI/CNF)₅ multilayer film. The authors suggest that the adsorption of catCNF onto the CNF network is not completely governed by electrostatics, but rather that there is a balance between a steric effect of stiff and highly crystalline nanofibrils inhibiting the adsorption and the electrostatic driving force promoting the adsorption. Eronen et al. (2012) could show using OCM-D that about the same amount of catCNFs deposits onto high and low charged CNFs. This result shows that nonelectrostatic interactions such as hydrogen bonding most probably play an important role in all cellulose multilayer systems.

In the case of the catCNF/CNCs system, QCM-D results show that a multilayer build-up can only be achieved if the adsorption density of the first CNF layer is high enough, i.e. under conditions where the catCNF are moderately charged (high pH conditions) or if the first CNF layer is spin coated (Olszewska et al. 2013).

Influence of the drying step

The presence of a drying step between each deposition step is a pivotal parameter for the growth of LbL films containing CNCs (*Fig 5*). When no drying step is applied, the film construction depends strongly on other parameters such as the salt concentration in the

polyelectrolyte solution, the CNC concentration and, to a lesser extent, the dipping time (Moreau et al. 2012). Additionally, the occurrence of a drying step gives thicker and more homogeneous films, displaying strong interference colors. Such strong drying effects might be related to the removal of water that leads to denser films and may promote hydrogen bonds between polymer chains and CNCs. The presence of hydrogen bonded networks also conveys more stability to the film. For example, in the absence of a drying step and at 1 M NaCl ionic strength for the polyelectrolyte solution, the construction of PAH/CNC films failed whatever the values of the other parameters (Moreau et al. 2012). However, under the same conditions, a regular growth of the films was achieved when drying was introduced after each deposition.

Under the same experimental conditions, using ellipsometry and optical reflectometry, Cranston et al. found that the multilayer buildup was linear, with an average thickness increase per bilayer of 2 nm and 16 nm for films prepared by solution dipping and spin coating, respectively (Cranston and Gray 2006). Considering the dimensions of CNCs, it seems that the film growth failed in the case of dipping when no drying step is present but succeeded for the spin coating method which by definition contains a drying phase during the spinning of the film. This thickness's difference can also be attributed to a more concentrated suspension since solvent is evaporated during spin coating or can be due to the lack of a PEI anchoring layer. Indeed, it seems that putting a PEI layer before the sequential adsorption of CNCs and polymers promotes a fast growth of the film.

Effect of adsorption time

Empirically chosen dipping times are in the range 10-20 min to allow for a two-step adsorption process: a fast initial adsorption of only few segments, followed by a rearrangement, relaxation and packing step. To confirm the fast adsorption of CNCs, Podsiadlo et al. (2007) have immersed a silicon wafer previously coated with PEI in a tunicin CNC suspension for a couple of seconds only.

Both AFM and SEM images revealed densely covered surfaces of CNCs with a porous architecture reminiscent

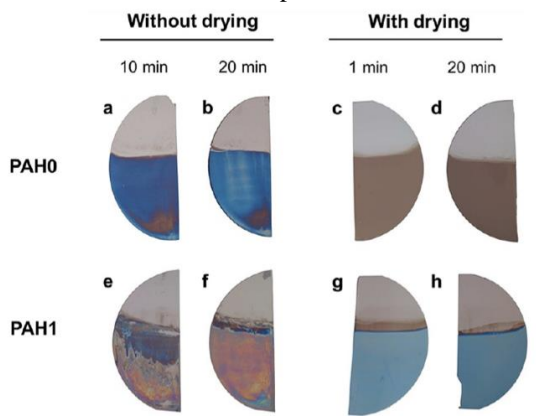


Fig 5 - Photos of (PAH/CNC)₈ films from (a–d) PAH0 (0 M NaCl) and (e–h) PAH1 (1 M NaCl) solutions constructed from dipping at (c,g) 1 min, (a,e) 10 min, and (b,d,f,h) 20 min adsorption dipping times, without or with a drying process. Reprinted with permission from Moreau et al. 2012. Copyright 2012 American Chemical Society.

of a flattened matchsticks pile. For short deposition times of 1 min, they obtained an average thickness increment per bilayer around 7 nm, which is in good agreement with other studies (Jean et al. 2009).

Due to the fast adsorption of the CNCs, the dipping time has little effect on the building of multilayers and on their internal structure. As an illustration, Jean et al. (2008) found the same thickness and the same dual-layer organization using 5, 10 or 15 min adsorption times and de Mesquita et al. (2010) stated that dipping times of 5 or 10 min give the same thickness for CNC/Chitosan multilayers.

Influence of the concentration

The influence of the CNC/CNF concentration on the architecture of the films depends on other parameters such as the deposition method and the presence of a drying step. When using the dipping method, the concentration seems to have an influence only if no drying step is applied. Indeed, the thickness increase per bilayer of dip-coated (PAH/CNC) multilayers made without drying step changes from 7-9 nm to 15-19 nm when the CNC concentration is increased from 0.5 wt% to 3.5 wt% (Moreau et al. 2012). Conversely, in the presence of a drying step, an increase in the CNC concentration also induces a thickness's increase, but the effect is less pronounced. For dip-coated CNF/PEI films, the adsorbed amount of CNF was found to be independent of the bulk CNF concentration in the investigated concentration range (0.015-0.25 wt%) (Aulin et al. 2008). When using spin-coating, Guyomard-Lack et al. (2012) reported a strong influence of the CNC concentration on the films growth since the thickness of a (CNC/XG)₈ film increased from 74 to 123 nm when increasing the concentration from 0.3 to 0.5 wt%.

Physical properties and functionalities of nanocellulose/ polymer thin films

Surface force measurements

For a deeper understanding of the multilayer behavior and of the interactions between film components, surface force measurements of various nanocellulose/polymer multilayers were carried out by colloidal probe atomic force microscopy under different solution conditions and using different probes (Aulin et al. 2010; Cranston et al. 2010; Eronen et al. 2012; Olszewska et al. 2013). Reported results generally show that the force response and the adhesive forces on separation are not solely governed by the capping layer but can significantly be affected by underlying layers, evidencing that interactions between LbL films are more complex than between single layers.

For example, it is shown in the exhaustive study of PAH/CNC multilayered films by Cranston et al. (2010) that the pre-contact normal forces between a silica probe and an CNC-capped multilayer film were monotonically repulsive at pH values where the material surfaces were similarly and fully charged. In contrast, at pH 3.5, the anionic surfaces were weakly charged but the underlying layer of cationic PAH was fully charged and attractive forces dominated due to polymer bridging from extended

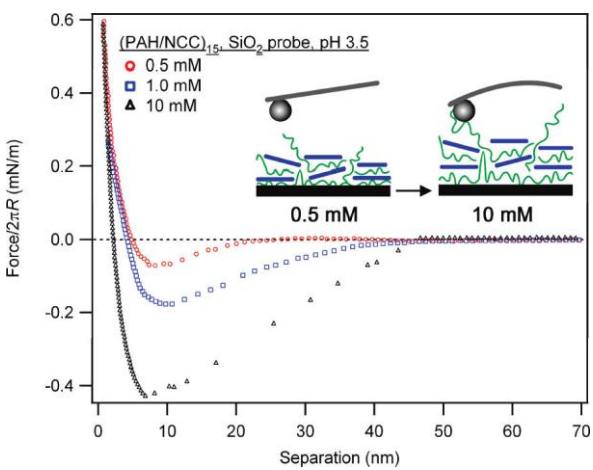


Fig 6 - Average normalized force-distance curves for the interaction of (PAH/CNC)15 and a silica probe at pH 3.5 and ionic strengths of 0.5 (circles), 1 (squares), and 10 mM (triangles). Inset shows a schematic representation of the PAH chains extending and bridging more at high ionic strength at an approximate separation distance of 40 nm (CNC: blue rods, PAH: green line, not drawn to scale). Reprinted with permission from Cranston et al. 2010. Copyright 2010 American Chemical Society.

PAH chains (*Fig 6*). The normalized forces between catCNF/CNC multilayers and cellulose sphere measured by Olszewska were also influenced by suspension pH and turned out to be more attractive at pH 4.5 than at pH 8.3, and the attraction was stronger when the capping layer was comprised of catCNF (Olszewska et al. 2013). Aulin et al. studied the forces acting between CNF multilayers in Milli-Q water. For catCNF/anCNF multilayers, low magnitude electrostatic forces dominate the interactions, due to the low adsorbed amount of moderately charged CNFs. In contrast, longer range forces resulting from a higher net charge were recorded for PEI/anCNF films. In all-cellulose films, the non-linearity of the curves also suggests that steric forces add to long range repulsive forces (Aulin et al. 2010; Eronen et al. 2012).

Mechanical properties

Although crystalline cellulose exhibits impressive mechanical properties, having a Young's modulus comparable to that of aramid fibers (Habibi et al. 2010), little information concerning the mechanical properties of nanocellulose thin films are found in the literature. However, a good understanding of these mechanical properties is of prime importance for the future application of cellulose multilayers in optical devices or functional coatings.

Direct measurements of the mechanical properties of nanocellulose/polymer thin films require the preparation of freestanding films that are not easy to obtain since a strong adhesion between the substrate and the film is often preferred to favor film's growth. Podsiadlo et al. (2007) recorded the stress-strain response of (PAH/tunicate CNCs) freestanding films under dry conditions. The porous 1 µm thick films exhibit a Young modulus around 6 GPa and an ultimate tensile strength as high as 110 MPa. The same experiment was performed by Karabulut and coworkers on (PEI/CNF)₁₅₀ films built

on a hydrophobic trichloro(1H,1H,2H,2H- perfluorooctyl)silane (PFOS)-coated silicon substrate and peeled off after drying using tweezers (2011). Interestingly, these authors showed that a minimal film thickness of 1-2 µm is compulsory to handle the samples for mechanical tests. The stress-strain curves are linear and do not show any plastic deformation, indicating that there is an effective bonding within the film and that CNFs' delamination occurs as the film is strained. Under absolute dry conditions, a Young's modulus of 9.3 GPa was found for the (PEI/CNF) films compared to 3.84 GPa for the solvent casted CNF films. The higher value might be due to the presence of the polymer that enables the CNFs to rearrange under stress and hence makes the film less brittle. However, it is expected that under higher relative humidity (RH) conditions PEI will have a negative effect on the mechanical properties of the film since it is known to soften at high RH.

To circumvent the difficulty in handling very thin films, the strain induced elastic buckling instability for mechanical measurements (SIEBIMM) technique can be used to determine the Young's modulus submicrometer nanocellulose multilayered films (Fig 7A) (Cranston et al. 2011; Eita et al. 2012, Kan, Cranston 2013). Tested on both CNF/PEI and CNC/PEI multilayers, Cranston et al. noticed that the film's thickness did not affect the value of the Young's modulus and more interestingly that humidity drastically modifies the mechanical properties of the films (Fig. 7A). For example, the Young's modulus of the (PEI/CNC) multilayers was 16, 12 and 3.5 GPa at 30%, 42% and 64% RH, respectively. The modulus PAH(PEI/CNF)_{15.5} film was found to be 17.2 GPa at 0% RH but decreased to 1.5 at 50% RH. This result emphasizes the fact that high mechanical properties could solely be reached under conditions where cellulosecellulose interactions are effective, i.e. when water absorption is avoided. Interestingly, the Young's modulus was larger at all relative humidity values for the (PEI/CNC) films than the (PEI/CNF) ones. The authors suggest that higher crystallinity, CNC volume fraction and PEI molecular weight (60 kDa for CNF/PEI films compared to 750 KDa for PEI/CNC) may enhance the mechanical properties of the films. Additionally, Eita et al. (2011) showed using SIEBIMM at 53% RH that the Young's modulus of polyvinyl amine (PVAm)/CNF multilayers doubled from 1.1 to 2.2 GPa upon introduction of silica particles in the film.

Brillouin light scattering is another technique that can be used directly on supported films and allows for the measurement of elastic constants at a microscopic level and in specific directions. Using this technique, Sui et al. (2010) could show that compared to pure polymer films, the presence of cotton CNCs increased the in-plane elastic constants of both (chitosan/CNC) (PDDA/CNC) LbL films by a factor of 2 and 3, respectively. The normal elastic constant increased by 50% in the case of PDDA/CNC but no effect was detected for chitosan/ CNC. Additionally, with increasing bilayers, the stiffness increased in the plane of the film at a higher rate than perpendicular to the film. In the case of

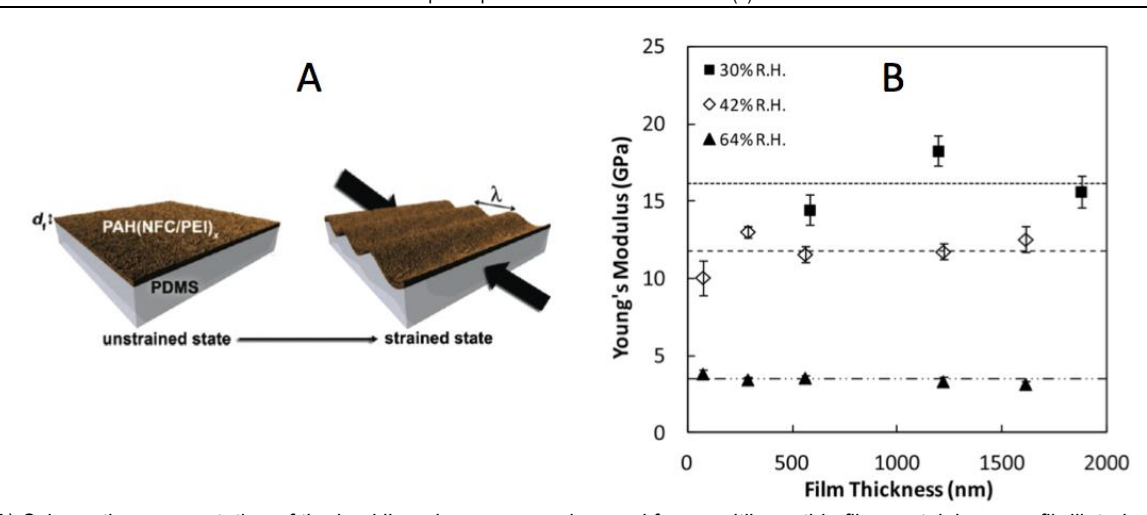


Fig 7 - A) Schematic representation of the buckling phenomenon observed for a multilayer thin film containing nanofibrillated cellulose (CNF) and polyethyleneimine (PEI) with a precursor layer of poly(allylamine hydrochloride) (PAH) on a compliant, PDMS, substrate. The variables d_i , the film thickness, and λ , the buckling wavelength are labeled in the diagram.B) Young's modulus, as calculated by strain-induced elastic buckling instability for mechanical measurement (SIEBIMM), for PAH(CNC/PEI)x films ranging in thickness from 61 nm to 1.7 μ m at (\blacksquare) 30% RH, (\diamondsuit) 42% RH, and (\blacktriangle) 64% RH. (Dotted lines show the average modulus value for the three relative humidity conditions). Reprinted with permission from Kan and Cranston 2013. Copyright 2013 TAPPI.

PDDA, the CNC/polymer interface seems to be more diffuse and nanorods deviate more from the in-plane orientation, so as to stretch across the interface and embed in the polymer layer, leading to a more efficient stress transfer within and across the layers. For the chitosan/CNC system, the interface should be better defined.

The LbL assembly technique was also used by Marais et al. (2013) to build PEI/CNF multilayers on the surface of pulp fibers in an attempt to improve the mechanical properties of paper sheets. A slow linear increase of the thickness as a function of the number of layers was observed and the amount of adsorbed polymer became very low after the first layer. Tensile tests measurements exhibited a surprising pattern where both the tensile index and the strain at break increased and decreased alternately upon adsorption of PEI and CNF, respectively. A similar effect was detected in the stress-strain curves. Quantitatively, the deposition of PEI/CNF on the fibers doubles the tensile index, from 20 Nm/g to 40 Nm/g, but was shown to be less efficient than the deposition of PAH/hyaluronic acid multilayers.

Optical properties

When built on reflective substrates like silicon wafers and above a given thickness, nanocellulose/polymer LbL films display angle-dependent intense colors (Fig 5) (Cranston and Gray 2006; Wågberg et al. 2008; Cerclier et al. 2011; Cerclier et al. 2011; Shariki et al. 2011; Dammak et al. 2013). These colors arise from interference between light reflected from the air/film interface and from the film/substrate interface. This property also demonstrates that the films are smooth enough to allow for a separation of the different colors from the white light spectrum. Thin film interference peaks can be monitored by optical reflectivity (Cranston and Gray 2006) and the color both depends on the thickness and mean refractive index of the LbL film. This property was used to design highly sensitive detectors for biomass hydrolysing enzymes and non-contact moistures

sensors (Cerclier et al. 2011; Granberg et al. 2012; Guyomard-Lack et al. 2012; Dammak et al. 2013) (see below).

Interestingly, Podsiadlo and coworkers (2007) reported the production of antireflective coatings from the assembly of tunicin CNCs and PEI in multilayered LbL films. Theoretically, an ideal antireflective thin film coating should meet two conditions: the refractive index of the thin film should be $(n_a \times n_s)^{0.5}$, where n_a and n_s are the refractive indices of air and substrate, respectively, and the thickness of the film should be $\lambda/4$, where λ is the wavelength of the incident light. In the case of glass or plastic as the substrate, n_s is about 1.5, which gives a refractive index of about 1.22 for the coating (n_{air}=1). Such conditions could be satisfied thanks to the highly porous structure architecture resulting from randomly oriented overlapping high aspect ratio nanocrystals. The onset of antireflection is reached with the deposition of the first bilayer, and the effect increases until 20 bilayers where a decrease in transparency and increase of light scattering is observed. At an optimum number of LbL deposition cycles, light transmittance reaches nearly 100% ($\lambda \sim 400$ nm) when deposited on a microscope glass slide and the refractive index is ~1.28 at $\lambda = 532$ nm. More recently, the optical properties of spincoated LbL films made of CNCs extracted from ramie fibers and lignin model compound (dehydrogenation polymer [DHP]) were measured by Hambardzumyan et al. (2011) in the visible wavelength range by ellipsometry and spectrophotometry. Results indicated that beyond six bilayers the LbL film exhibited antireflective properties.

Advanced functionalities towards applications

Thanks to their tunable architecture and/or the introduction of active components, nanocellulose/polymer multilayered film can achieve different functionalities that pave the way to applications in various fields. Below are some examples of functional films based on tailored architectures.

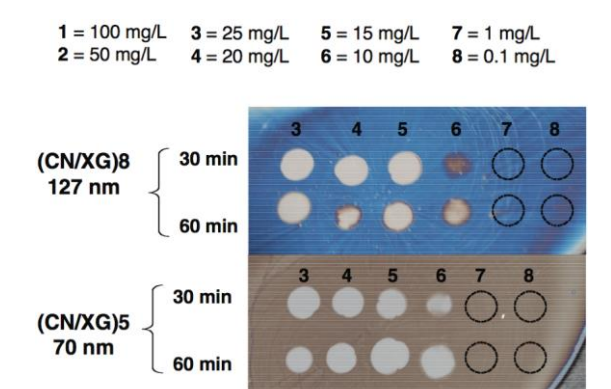


Fig 8 - Enzyme-induced degradation images of thin films composed of 5 CNC/XG bilayers and 8 CNC/XG bilayers after 30 and 60 min for different enzyme concentrations listed at the top of the figure. Reprinted with permission from Cerclier et al. 2011a. Copyright 2011 Wiley-VCH Verlag Gmbh & Co.

Biomass hydrolysing enzymes detection

The production of biofuels from plant biomass degradation requires the development of easy-to-use, sensitive and rapid screening tests, applicable to a wide range of hydrolytic enzymes. In this framework, Cerclier et al. took advantage of the interference colors displayed by fully biosourced (CNC/XG) LbL films to design highly sensitive detectors for biomass-hydrolyzing enzymes based on a simple principle (Cerclier et al. 2011; Guyomard-Lack et al. 2012; Cerclier et al. 2013). Indeed, when cellulolytic enzymes mixtures are deposited on a thin CNC/XG LbL film initially exhibiting an intense color, the enzymatic degradation induces a decrease in the film thickness that locally gives rise to color changes, which can easily be detected by the naked eye (Fig 8). This qualitative enzymatic assay method appeared to be easy to use, fast and about 150 times more sensitive than a standard method (Cerclier et al. 2011). Similarly, structural colors were obtained by assembling CNCs with cationic xylans into multilayered films (Dammak et al. 2013). These films were shown to be appropriate for the detection of xylanase activity, though the assay sensitivity was found to be only similar to that of a usual colorimetric test.

Tuning percolation speed in polyaniline–nanocellulose films

CNFs extracted from sisal have been assembled with polyaniline on tin-doped indium oxide (ITO) substrates to form electrochemically active films (Shariki et al. 2011). The propagation of the charges in these nanocomposite films was investigated and shown to be architecture dependent. Interestingly, the number of layers causes a systematic change in the voltammetric response and very thin films of only one or 2 layers deposited on ITO exhibited two prominent redox processes. Results also suggest that the pure polyaniline film is switching approximately two order of magnitude faster compared to the polyaniline/nanocellulose film. The authors infer that the electrically conducting emeraldine phase is formed even when a low amount of polyaniline is present in pores between CNFs and that electrical phenomena such as the propagation rate can be tuned based on the polyaniline content and the nanoarchitecture of the

multilayers. Additionally, the LbL films displayed a catalytic activity.

Introduction of temperature responsiveness

Stimuli-responsive nanocomposites are of great interest for the controlled release of active molecules or the tunable interactions at interfaces. In this framework, Utsel and coworkers have synthetized a block copolymer in which one block is a positively charged and weakly thermosensitive copolymer of poly isopropylacrylamide) (PNIPAAm) and (3-acrylamidopropyl) trimethylammonium chloride (APTAC), while the other block is a neutral block of the homopolymer polyNIPAAm with strong thermoresponsive properties (Utsel et al. 2010). Multilayers could be formed with this polymer and CNFs but limitations in the number of stable layers that could be assembled were observed, probably due to the fact that non-adsorbed neutral NIPAM segments restrain the electrostatic interactions between the copolymer and the CNFs. Successful exponential film growth was achieved when a PEI layer was intercalated between two successive copolymer/CNF bilayers. The copolymer/CNF multilayers exhibited thermosensitivity and the temperature effect was stronger when PEI was incorporated. Such thermoresponsive LbL films could be used for the design of drug delivery systems or as membranes with temperature dependent permeability.

Transparent films with gas barrier properties

Due to its renewable character and its inherent gas barrier properties, nanocellulose is receiving increasing attention for the replacement of petroleum derived polymers in gas barrier devices. In this context, Aulin et al. (2013) used the LbL strategy to build (CNF/PEI) multilayers on poly (lactic acid) (PLA) flexible substrates. The resulting multilayer-coated films exhibited significantly increased oxygen and water vapor barrier properties, which outperform those of pure solvent-casted CNF films. For example, the oxygen permeability is equal to 0.34 and 0.71 cm³μm/m²daykPa for (PEI/CNF)₅₀ multilayers and solvent casted-NFC films, respectively. The LbL-coated PLA substrates were also found to be less moisture sensitive than pure PLA. In addition to their high gas barrier properties, these thin films assemblies exhibit a remarkable optical transparency, which is close to that of pure PLA films, and possess a strong flexibility. These features make them promising candidates for large-scale applications in food packaging or flexible electronics.

Wet-stable adhesive films

Dopamine functionalized CNFs (DOPA-CNF) were used in association with PEI to build LbL film in an attempt to mimic mussel adhesion on solid substrates (Karabulut et al. 2012). QCM-D monitoring of film growth shows comparable adsorbed mass for four-bilayers DOPA-CNF/PEI and unmodified CNF/PEI films, even if the CNF modification resulted in a lower charge density. However, 3 times higher dissipation values were recorded for DOPA-CNF/PEI, showing that softer films were obtained with this system. The thickness of dry (DOPA-CNF/PEI)₈ films of 130 nm increased 3 times upon injection of water and the swelling of the film increased even more in presence of a FeCl₃ solution, due to the

formation of ionic coordination complexes and due to decreased interactions between DOPA-CNF and PEI. Wet adhesion of DOPA-CNF/PEI LbL films to a silica probe in the presence of Fe³⁺ ions was monitored by AFM force measurements and found to be much stronger than when unmodified CNFs are used, demonstrating that chemical modification of nanocellulose gives rise to LbL nanocoatings with new functionalities.

Conclusions

The layer-by-layer assembly technique is a simple and versatile tool to build a wide variety of nanocellulose/ polymer multilayered films with a tunable architecture. The final structure of the films is governed by the individual properties of the constituents, the interactions forces between the nanocellulose and the polymer and the deposition method parameters. The use of needle-shaped CNCs or high aspect ratio flexible CNFs gives rise to multilayers displaying different organizations and thickness increments due to their dissimilar morphology and charge densities. The successive layer adsorption can be achieved through electrostatic interactions, but can also arise from H-bonds or van der Waals interactions, which enables the association with either linear or branched synthetic polycations or neutral biopolymers. The specific exceptional properties of both types of nanocellulose combined with the ability to finely tailor the nanoarchitecture of the film provide ways to design high performance free-standing films or coatings with advanced properties. It is to be expected that future innovations in the field will rely on the introduction of functional components, e.g. stimuli-responsive species, and use of chemically modified nanocellulose. The construction of hybrid organic/inorganic systems should also impart new properties. It can finally be anticipated that nanocellulose-based multilayers will successfully be used in the fields of materials separation, flexible electronics, bioenergy, advanced optical coatings or in the biomedical area.

Acknowledgements

CM and BJ are grateful to Laurent Heux (CERMAV) and Erik Watkins (ILL) for valuable help in the editing of the manuscript.

Literature

- Aulin, C., Ahola, S., Josefsson, P., Nishino, T., Hirose, Y., Österberg, M. and Wågberg, L. (2009): Nanoscale Cellulose Films with Different Crystallinities and Mesostructures-Their Surface Properties and Interaction with Water, Langmuir, 25, 7675-7685.
- Aulin, C., Johansson, E., Wågberg, L. and Lindström, T. (2010): Self-Organized Films from Cellulose I Nanofibrils Using the layer-by-layer Technique, Biomacromolecules, 11, 872-882.
- Aulin, C., Karabulut, E., Tran, A., Wågberg, L. and Lindström, T. (2013): Transparent Nanocellulosic Multilayer Thin Films on Polylactic Acid with Tunable Gas Barrier Properties, ACS Appl. Mater. Interfaces, 5, 7352-7359.
- Aulin, C., Varga, I., Claesson, P. M., Wågberg, L. and Lindström, T. (2008): Buildup of Polyelectrolyte Multilayers of Polyethyleneimine and Microfibrillated Cellulose Studied by in Situ Dual-Polarization Interferometry and Quartz Crystal Microbalance with Dissipation, Langmuir, 24, 2509-2518.

- Cerclier, C., Cousin, F., Bizot, H., Moreau, C. and Cathala, B. (2010): Elaboration of Spin-Coated Cellulose-Xyloglucan Multilayered Thin Films, Langmuir, 26, 17248-17255.
- Cerclier, C., Guyomard-Lack, A., Moreau, C., Cousin, F., Beury, N., Bonnin, E., Jean, B. and Cathala, B. (2011): Coloured Semi-reflective Thin Films for Biomass-hydrolyzing Enzyme Detection, Advanced Materials, 23, 3791-3795.
- Cerclier, C. V., Guyomard-Lack, A., Cousin, F., Jean, B., Bonnin, E., Cathala, B. and Moreau, C. (2013): Xyloglucan-Cellulose Nanocrystal Multilayered Films: Effect of Film Architecture on Enzymatic Hydrolysis, Biomacromolecules, 14, 3599-3609.
- Cranston, E. D., Eita, M., Johansson, E., Netrval, J., Salajkova, M., Arwin, H. and Wågberg, L. (2011): Determination of Young's Modulus for Nanofibrillated Cellulose Multilayer Thin Films Using Buckling Mechanics, Biomacromolecules, 12, 961-969.
- **Cranston, E. D. and Gray, D. G.** (2006a): Morphological and optical characterization of polyelectrolyte multilayers incorporating nanocrystalline cellulose, Biomacromolecules, 7, 2522-2530.
- Cranston, E. D. and Gray, D. G. (2006b): Formation of cellulose-based electrostatic layer-by-layer films in a magnetic field, Sci. Technol. Adv. Mater., 7, 319-321.
- **Cranston, E. D. and Gray, D. G.** (2008): Birefringence in spin-coated films containing cellulose nanocrystals, Colloids Surf., A, 325, 44-51.
- Cranston, E. D., Gray, D. G. and Rutland, M. W. (2010): Direct Surface Force Measurements of Polyelectrolyte Multilayer Films Containing Nanocrystalline Cellulose, Langmuir, 26, 17190-17197.
- Dammak, A., Moreau, C., Beury, N., Schwikal, K., Winter, H. T., Bonnin, E., Saake, B. and Cathala, B. (2013): Elaboration of multilayered thin films based on cellulose nanocrystals and cationic xylans: application to xylanase activity detection, Holzforschung, 67, 579-586.
- de Mesquita, J. P., Donnici, C. L. and Pereira, F. V. (2010): Biobased Nanocomposites from layer-by-layer Assembly of Cellulose Nanowhiskers with Chitosan, Biomacromolecules, 11, 473-480.
- de Mesquita, J. P., Patricio, P. S., Donnici, C. L., Petri, D. F. S., de, O. L. C. A. and Pereira, F. V. (2011): Hybrid layer-by-layer assembly based on animal and vegetable structural materials: multilayered films of collagen and cellulose nanowhiskers, Soft Matter, 7, 4405-4413.
- **Decher, G.** (1997): Fuzzy nanoassemblies: Toward layered polymeric multicomposites, Science, 277, 1232-1237.
- **Decher, G., Hong, J. D. and Schmitt, J.** (1992): Buildup Of Ultrathin Multilayer Films By A Self-Assembly Process .3. Consecutively Alternating Adsorption Of Anionic And Cationic Polyelectrolytes On Charged Surfaces, Thin Solid Films, 210, 831-835.
- **Decher, G., Schlenoff, J. B.** and Editors (2012): Multilayer Thin Films: Sequential Assembly of Nanocomposite Materials, Second Edition.
- **Eichhorn, S. J.** (2011): Cellulose nanowhiskers: promising materials for advanced applications, Soft Matter, 7, 303-315.
- **Eita, M., Arwin, H., Granberg, H. and Wågberg, L.** (2011): Addition of silica nanoparticles to tailor the mechanical

- properties of nanofibrillated cellulose thin films, J. Colloid Interface Sci., 363, 566-572.
- Elazzouzi-Hafraoui, S., Nishiyama, Y., Putaux, J. L., Heux, L., Dubreuil, F. and Rochas, C. (2008): The shape and size distribution of crystalline nanoparticles prepared by acid hydrolysis of native cellulose, Biomacromolecules, 9, 57-65.
- **Eronen, P., Laine, J., Ruokolainen, J. and Österberg, M.** (2012): Comparison of Multilayer Formation Between Different Cellulose Nanofibrils and Cationic Polymers, J. Colloid Interface Sci., 373, 84-93.
- Granberg, H., Coppel, L. G., Eita, M., de Mayolo, E. A., Arwin, H. and Wågberg, L. (2012): Dynamics of moisture interaction with polyelectrolyte multilayers containing nanofibrillated cellulose, Nordic Pulp & Paper Research Journal, 27, 496-499.
- Guyomard-Lack, A., Cerclier, C., Beury, N., Jean, B., Cousin, F., Moreau, C. and Cathala, B. (2012): Nanostructured cellulose nanocrystals-xyloglucan multilayered films for the detection of cellulase activity, European Physical Journal-Special Topics, 213, 291-294.
- **Habibi, Y., Lucia, L. A. and Rojas, O. J.** (2010): Cellulose Nanocrystals: Chemistry, Self-Assembly, and Applications, Chemical Reviews, 110, 3479-3500.
- Hambardzumyan, A., Molinari, M., Dumelie, N., Foulon, L., Habrant, A., Chabbert, B. and Aguie-Beghin, V. (2011): Structure and optical properties of plant cell wall bio-inspired materials: Cellulose-lignin multilayer nanocomposites, C. R. Biol., 334, 839-850.
- Hanus, J. and Mazeau, K. (2006): The xyloglucan-cellulose assembly at the atomic scale, Biopolymers, 82, 59-73.
- **Iler, R.K.** (1966): Multilayers of colloidal particles, J. Colloid Interface Sci., 21, 569-594
- **Jean, B., Dubreuil, F., Heux, L. and Cousin, F.** (2008): Structural Details of Cellulose Nanocrystals/Polyelectrolytes Multilayers Probed by Neutron Reflectivity and AFM, Langmuir, 24, 3452-3458.
- Jean, B., Heux, L., Dubreuil, F., Chambat, G. and Cousin, F. (2009): Non-Electrostatic Building of Biomimetic Cellulose-Xyloglucan Multilayers, Langmuir, 25, 3920-3923.
- Kan, K. H. M. and Cranston, E. D. (2013): Mechanical testing of thin film nanocellulose composites using buckling mechanics, Tappi J., 12, 9-17.
- **Karabulut, E., Pettersson, T., Ankerfors, M. and Wågberg, L.** (2012): Adhesive layer-by-layer Films of Carboxymethylated Cellulose Nanofibril Dopamine Covalent Bioconjugates Inspired by Marine Mussel Threads, Acs Nano, 6, 4731-4739.
- **Karabulut, E. and Wågberg, L.** (2011): Design and characterization of cellulose nanofibril-based freestanding films prepared by layer-by-layer deposition technique, Soft Matter, 7, 3467-3474.
- Klemm, D., Kramer, F., Moritz, S., Lindstrom, T., Ankerfors, M., Gray, D. and Dorris, A. (2011): Nanocelluloses: A New Family of Nature-Based Materials, Angewandte Chemie-International Edition, 50, 5438-5466.
- Marais, A., Utsel, S., Gustafsson, E. and Wågberg, L. (2013): Towards a super-strainable paper using the layer-by-layer technique, Carbohydr. Polym., Ahead of Print.

- Moreau, C., Beury, N., Delorme, N. and Cathala, B. (2012): Tuning the Architecture of Cellulose Nanocrystal-Poly(allylamine hydrochloride) Multilayered Thin Films: Influence of Dipping Parameters, Langmuir, 28, 10425-10436.
- Oksman, K. M., Aji P.; Bismarck, A.; Rojas, O.; Sain, M.; Editors. Handbook of Green Materials: processing technologies, properties and applications, World Scientific Publishing, in press.
- Olszewska, A. M., Kontturi, E., Laine, J. and Österberg, M. (2013): All-cellulose multilayers: long nanofibrils assembled with short nanocrystals, Cellulose (Dordrecht, Neth.), 20, 1777-1789.
- Pääkkö, M., Ankerfors, M., Kosonen, H., Nykanen, A., Ahola, S., Österberg, M., Ruokolainen, J., Laine, J., Larsson, P. T., Ikkala, O. and Lindström, T. (2007): Enzymatic hydrolysis combined with mechanical shearing and high-pressure homogenization for nanoscale cellulose fibrils and strong gels, Biomacromolecules, 8, 1934-1941.
- Podsiadlo, P., Choi, S.-Y., Shim, B., Lee, J., Cuddihy, M. and Kotov, N. A. (2005): Molecularly Engineered Nanocomposites: Layer-by-Layer Assembly of Cellulose Nanocrystals, Biomacromolecules, 6, 2914-2918.
- Podsiadlo, P., Sui, L., Elkasabi, Y., Burgardt, P., Lee, J., Miryala, A., Kusumaatmaja, W., Carman, M. R., Shtein, M., Kieffer, J., Lahann, J. and Kotov, N. A. (2007): layer-by-layer Assembled Films of Cellulose Nanowires with Antireflective Properties, Langmuir, 23, 7901-7906.
- Revol, J. F., Bradford, H., Giasson, J., Marchessault, R. H. and Gray, D. G. (1992): Helicoidal self-ordering of cellulose microfibrils in aqueous suspension, International Journal of Biological Macromolecules, 14, 170-172.
- Shariki, S., Liew, S. Y., Thielemans, W., Walsh, D. A., Cummings, C. Y., Rassaei, L., Wasbrough, M. J., Edler, K. J., Bonne, M. J. and Marken, F. (2011): Tuning percolation speed in layer-by-layer assembled polyaniline-nanocellulose composite films, J. Solid State Electrochem., 15, 2675-2681.
- **Sui, L., Huang, L., Podsiadlo, P., Kotov, N. A. and Kieffer, J.** (2010): Brillouin Light Scattering Investigation of the Mechanical Properties of layer-by-layer Assembled Cellulose Nanocrystal Films, Macromolecules, 43, 9541-9548.
- **Turbak, A. F., Snyder, F. W. and Sandberg, K. R.** (1983): Microfibrillated cellulose, a new cellulose product: properties, uses, and commercial potential, J. Appl. Polym. Sci. Appl. Polym. Symp., 37, 815-27.
- **Utsel, S., Malmström, E. E., Carlmark, A. and Wågberg, L.** (2010): Thermoresponsive nanocomposites from multilayers of nanofibrillated cellulose and specially designed N-isopropylacrylamide based polymers, Soft Matter, 6, 342-352.
- Wågberg, L., Decher, G., Norgren, M., Lindström, T., Ankerfors, M. and Axnas, K. (2008): The build-up of polyelectrolyte multilayers of microfibrillated cellulose and cationic polyelectrolytes, Langmuir, 24, 784-795.
 - Manuscript received December 11, 2013 Accepted January 6, 2013